Enhancement of the Utilization of Electric Vehicle Charging Stations in a Commercial Distribution Network

Willy Stephen Tounsi Fokui[1,*], *Ebunle Akupan Rene*[2], *Danube Kirt Ngongang Wandji*[3]

[1]Teleconnect GmbH, Am Lehmberg 54, 01157 Dresden, Germany
[2]University of New Hampshire, 105 Main St, Durham, NH 03824, United States of America
[3]Stockholm Environment Institute Africa, Nairobi, Kenya

*Corresponding Author: Willy Stephen Tounsi Fokui (email: willysytis@gmail.com)
(Received: 05-August-2025; accepted: 31-October-2025; published: 31-December-2025)
http://dx.doi.org/10.55579/jaec.202594.512

Abstract. *The high dependence of the transport sector on fossil fuels has raised serious concerns worldwide. It accounts for most greenhouse gas (GHG) emissions in many countries and is a major driver of climate change and air pollution, both of which affect health and the environment. Reducing carbon dioxide (CO2) emissions in this sector is urgently needed, along with measures to increase resilience to climate change. One promising solution is the adoption of electric vehicles (EVs), which produce no emissions. However, the benefits of EVs depend on installing enough EV charging stations (EVCSs) where people live, work, and play. Charging EVs from the electrical distribution network (DN) adds extra load, so optimal placement of EVCSs is essential to serve the EV population efficiently. Integrating distributed generation (DG) into the DN can help mitigate the negative impact of EVs, but it must be done carefully to avoid exceeding grid capacity. To address these challenges, the hybrid Bacterial Foraging Optimization - Particle Swarm Optimization (BFO-PSO) technique is proposed for effectively allocating EVCSs alongside photovoltaic (PV) systems within the DN. This approach aims to reduce power loss and the average voltage deviation index while improving voltage profile and stability. The study utilizes the standard IEEE 69-node test distribution network (DN), modelled as a purely commercial network comprising retail shops, marketplaces, and offices. Simulation results show the effectiveness of the BFO-PSO in optimally integrating the EVCSs and the compensating PV systems into the distribution network. For example, without EVCSs and PVs, the network's power loss was 138.89 kW. This slightly increased to 142.99 kW with EVCSs but decreased significantly to 48.64 kW when PV systems were added. To verify the effectiveness of the hybrid BFO-PSO, results were compared with those obtained when each optimization, PSO and BFO, is used standalone for the same task, confirming its superiority. The successful integration of EVCSs and PV systems in current distribution networks will depend on coordinated efforts between the transport sector and utility companies.*

Keywords: *BFO-PSO, Greenhouse gas, Electric vehicles, Photovoltaic, Charging stations.*

1.0 Introduction

As a result of the enormous greenhouse gas (GHG) release coming from the field of transportation, electric vehicles (EVs) are quickly being adopted in many nations worldwide as a substitute for petroleum-based cars [1]. The fast endorsement of EVs today is also due to the increasing exhaustion of crude oil, as well as the impact it has on the environment [2]. Consequently, the rapid propagation of EVs, which are tranquil and free from emissions [3]. Despite the sales of electric cars having dramatically increased over the years, these are primarily concentrated in the developed world, such as Europe, the United States of America, and China [4]. Developing countries are still significantly lagging, but several countries like Kenya are putting in numerous efforts to increase their EV fleets. Nowadays, it is very easy to find public transportation EVs like e-buses, taxis, e-bikes, etc, in large cities like Nairobi. One of the challenges in the uptake of EVs is the ease of access to charging facilities where people work and live, as the rapid increase in the number of EVs relies on the fast growth of these charging facilities [5]. EV chargers can be placed into three categories, Level 1, 2, and 3, with Level 3 being the fastest, having the capability of fully charging an EV within an hour [6].

The substitution of conventional vehicles with EVs benefits not only the environment but the power distribution network (DN) as well, as the EVs could aid in voltage/frequency support and spinning reserve to take charge of generation loss or sudden load increase [7]. Notwithstanding, the misappropriation of EVs in the DN could be fatal in terms of voltage variation away from permitted limits, power loss increase, and power quality degradation [8]. This disagreeable impact could be remedied by optimally sizing and allocating distributed generations (DGs) [9]. Distributed generation is the generation of electricity at load centers [10]. The most environmentally friendly and sustainable distributed electricity generation technology of recent years is solar photovoltaic [11]. Photovoltaic (PV) systems have become the most distinguished DG because of the continuous drop in the cost of PV panels and accompanying components, with the massive energy from the sun being a major factor [12]. The installation rate of PVs worldwide is more than 70 GW per year [13]. PV systems could mitigate the adverse effects of EVs in the DN through voltage support and peak shaving [14].

The accelerated multiplication of EVs in today's transportation area has resulted in countless research works on the delicate fitting of EV charging stations (EVCSs) in the DN. Some research focuses on dynamic parameters, such as the driving patterns of EV owners, the EV battery, arrival times, and departure times, among others. Meanwhile, other research works focus mainly on placing the EVCS in the DN, looking at the EVCS as static loads. P. V. K. Babu and K. Swarnasri in [15] optimally placed EVCSs in the DN, accompanied by DGs using Harries Hawk Optimization (HHO) and Teaching-Learning Based Optimization (TLBO), with the optimization problem minimizing power loss, average voltage deviation index, and maximizing voltage stability index. The authors went further to optimally size and site DGs to reduce the impact of the EVCSs on the network. They used the IEEE 33 and 69 bus test DNs to test their proposed solution. The results obtained showed that the HHO could find better locations for the EVCSs and the DGs compared to the TLBO. The authors did not hybridize both techniques to see whether it would yield the best results compared to using both techniques separately. E. A. Rene et al. in [16] used the hybrid Genetic Algorithm and Particle Swarm Optimization (GA-PSO) to allocate EVCSs in a DN with high penetration of DGs (60% penetration), with the objective being power loss minimization and voltage deviation index improvement. The model was tested on the standard IEEE 33 and 69 node test feeders, and the results demonstrated the effectiveness of the proposed method. Notwithstanding, considering PV systems as DG, the daytime variation of PV production of the PV systems was not considered. The PV systems were studied as static generation systems producing constant power at a power factor of 0.95. In [17], Levels 1, 2, and 3 chargers were optimally placed by M. Z. Zeb et al. to effectively manage EV loads while minimizing the cost of installation of the charging

stations, the loading of the distribution transformers, and losses. The EVs were modeled as stochastic loads as a result of the uncertain nature of the EV users, and the proposed method was validated on the DN of the National University of Sciences and Technology (NUST), Pakistan. PVs were also integrated to limit the adverse impact of the EVs on the DN. Despite the PSO being able to solve the problem at hand, PSO has an issue of being stuck on the local minimum solution and therefore never obtaining the global solution. In [18], Genetic Algorithm (GA) was proposed by S. Pazouki et al. for planning EV charging stations in a DN with capacitors to reduce power loss and boost voltage, with the IEEE 34 bus radial DN used as a test network. GA was able to suitably integrate the EVCSs and capacitors in the DN. Notwithstanding, GA, when used standalone, has well-known issues like slow and premature convergence, parameter sensitivity, and a lack of assurance that the global solution will be found. S. K. Injeti and V. K. Thunuguntla used Particle Swarm Optimization (PSO) and Butterfly Optimization (BO) techniques in [19] to integrate DGs in the DN in the presence of EVs to solve the multi-objective optimization problem to reduce daily power loss and enhance the DN's voltage characteristics. The test network used was the IEEE 33-node DN, and the simulation results demonstrated the superiority of the BO over PSO in solving the optimization problem. It would have been interesting to hybridize both techniques and investigate the strengths of the resulting hybrid in solving the problem at hand. Using a metropolitan test network, S. Nugraha et al. in [20] used the hybrid Genetic Algorithm-Modified Salp Swarm Algorithm (HGAMSSA) to size and site EVCSs in the DN with PVs to minimize the impact on power loss, voltage, and overload. Three scenarios were considered to find the optimal size and location of the EVCSs: the first being that the EVCSs were a mixture of Level 1, 2, and 3 chargers, the second scenario considered the EVCS to be Level 2 and 3 chargers, and the third considered the EVCSs to be only Level 3 chargers. The overall simulation results demonstrated the capability of the network to be optimized by at least 75.53% when the EVs interact with the grid in grid-to-vehicle (G2V) mode. M. Bilal et al. in [21] used the hybrid Grey Wolf-Particle Swarm Optimization (GWOPSO) technique to allocate EVCSs and DGs in the DN to maintain the system reliability within limits, with the IEEE 33 and 69 node test feeders used as test networks. The DGs used in this study are at a unity power factor, meaning they did not inject reactive power into the network. In the research paper [22], S. Deb et al., the focus was on allocating EVCSs using a Pareto dominance-based hybrid Chicken Swarm Optimization (CSO) and TLBO, minimizing the cost of the EVCSs, while ensuring sufficient grid stability, and the accessibility of the EVCSs to the EV users. The results obtained showed that the combination of CSO and TLBO could produce promising results, and it was demonstrated to be effective in addressing the practical problem of charging station placement.

This work proposes a hybrid Bacterial Foraging Optimization - Particle Swarm Optimization (BFO-PSO) technique to effectively distribute electric vehicle charging stations (EVCSs) in a commercial DN to service the EV fleet (taxis, private cars) during peak periods. To enhance the utilization of the EVCSs, it strategically inserts distributed PV systems to remedy the adverse effects of massive EV charging on the DN. The optimization problem is elaborated as a multi-objective function minimizing power loss and average voltage deviation index while enhancing the voltage stability index of the network. The contribution of this paper includes,

- Solving the placement of the EVCSs in a purely commercial DN using the hybrid BFO-PSO, considering that EV users charge their EVs during peak load hours from 10 am to 3 pm daily.

- Using the hybrid BFO-PSO to optimally size and integrate compensating PV systems into the DN with the EVCSs to alleviate the adverse impacts of the EVs on the DN during peak load hours, which also corresponds to peak sun hours, hence peak PV production hours. In so doing, enhance the full utilization of the EVCSs.

This paper's remaining sections are arranged as follows: the methodology comes next, then

the findings and discussions, and finally the conclusion.

2.0 Methodology

2.1 Test Distribution Network

The test network utilized in this study is the standard IEEE 69-node DN, shown in Fig. 1. Its nominal voltage is 12.66 kV, and it is balanced. The total demand of the network is shown in Table 1 as obtained from [23]. In this study, the DN is a purely commercial DN with retail shops, marketplaces, and offices, with its normalized daily load curve obtained from [24], as shown in Fig. 2, the daily solar irradiance obtained from [25], and shown in Fig. 3.

Tab. 1: IEEE 69 bus power demand

Active Power (kW)	Reactive Power (kVAr)	Apparent Power (kVA)
3801.4	2693.6	4658.98

2.2 Estimation of the EV Population

An estimate of the number of business entities in the study network is needed to estimate the EV population. Assuming every business unit in the study network has an average three-phase power demand of 5 kVA, the number of business entities is therefore calculated to be approximately 932. Considering that an average of 5 people work in each business entity, the number of people in the area is 4660. Amongst all these people working in this study area, 20 own EVs, work in different business entities, and charge them while at work.

The number of EV taxis that service the customers visiting the business entities daily needs to be estimated. To do this, it is estimated that an average of 100,000 customers visit daily, and that 180 EVs are used to move people from one point to another and need to be charged regularly. This, therefore, means that the study area has a total EV fleet of 200 EVs.

2.3 EV Power Demand

It is considered that the EV population (privately owned and taxis) is a mixture of 4 different models of battery electric vehicles, as shown in Table 2. To service the EV population, 152

Tab. 2: EV Models and Quantities [2]

EV Model	Battery Specifications	Charging Point
Volkswagen e-UP!	32.3kWh	3-phase 32A (22kW)
Peugeot e-208	45.0kWh	3-phase 32A (22kW)
Mazda MX-30	30kWh	3-phase 32A (22kW)
Hyundai IONIQ Electric	38.3kWh	3-phase 32A (22kW)

EV charging points (CPs) will be strategically installed across 5 EVCSs in the network. All the CPs consist of Level 2 chargers, as they are faster and more efficient than Level 1 chargers, and will stress the DN less compared to Level 3 chargers. The number of CPs and the power rating of each EVCS are shown in Table 3. All the 200 EVs in the study area are not expected to be charged simultaneously. A maximum of 152 could be charged at the same time.

Tab. 3: Characteristics of EVCS and the number of CP

	Rating per CP (kW)	Number of CP	Rating of EVCS (kW)
EVCS 1	22	20	440
EVCS 2	22	25	550
EVCS 3	22	40	880
EVCS 4	22	35	770
EVCS 5	22	32	704
TOTAL		152	3344

According to [26], from the viewpoint of the DN, an EV can be seen as:

- A straightforward load that draws steady power from the network when charging. This is usually uncontrolled EV charging, wherein the EV battery is charged with a constant current when the EV is plugged

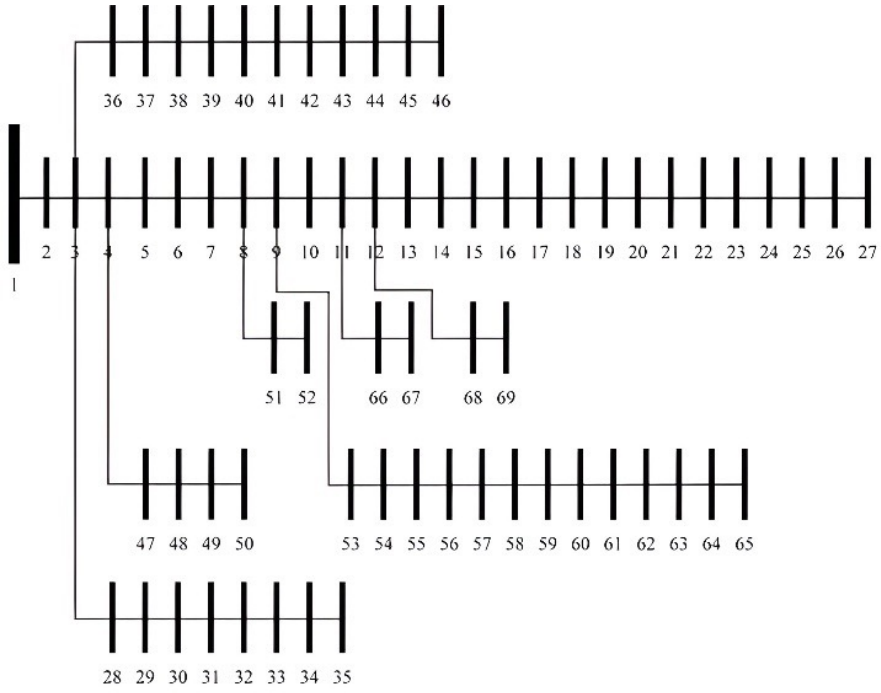

Fig. 1: IEEE 69 bus DN

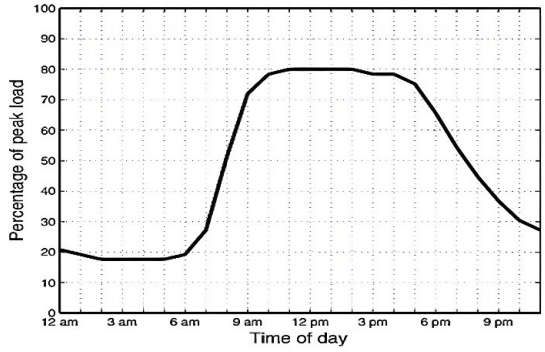

Fig. 2: Normalized daily load profile of the study area [22]

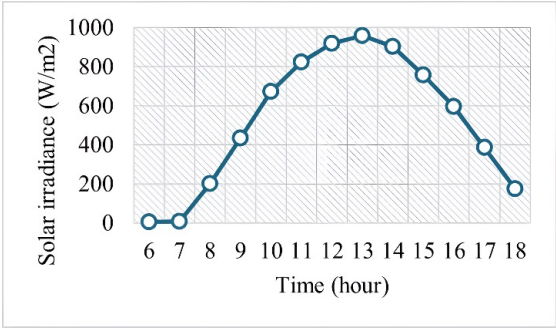

Fig. 3: Average daily solar irradiance

into a CP in an EVCS. This is called grid-to-vehicle (G2V).

- A power bank that discharges (vehicle-to-grid (V2G)) and charges (G2V) as per the network conditions. Here, the charging point is designed to operate in two directions and is equipped with a regulatory system that determines the direction of power flow based on the network condition. Therefore, the EV could be used as a spinning reserve and voltage/frequency regulator for valley filling and peak shaving.

- A compounded load whose charging period can be adjusted. This is another form of controlled EV charging wherein the EV is only charged during favorable network conditions.

In this study, the EVs are considered per option one above, which is a straightforward load

that draws steady power from the network when charging.

2.4 PV System Characteristics

The PV systems, optimally sized and placed to alleviate the adverse impact of the EVCSs on the network, are modeled as negative PQ loads. To incorporate the capability of the PV inverters to feed reactive power into the network, the PVs are modeled at a power factor of 0.95. Five (5) PV systems are used for compensation.

2.5 Assumptions and considerations

The following assumptions and considerations are made in this study:

- The EVs are static loads that draw constant power from the DN when plugged into a CP.
- The EV battery state of charge, arrival time, and departure time are not considered.
- All CPs are equipped with Level 2 chargers, and therefore, the EV owners have no charging preferences.
- All the 152 CPs are fully utilized during peak load hours (from 10 am to 3 pm).
- The PV systems deliver rated power to the distribution network during peak sun periods.
- The intermittent behaviour of PV systems is not considered.
- The PV systems do not have storage capabilities and therefore feed all their power to the grid.

2.6 Optimal Allocation of the EVCSs and the PV Systems

2.6.1 Formulation of the Optimization Problem

The optimization problem is constructed as an overall minimization problem.

a. Power loss minimization

$$f_i(a) = min \sum_{a=1}^{br} R_{br} * I_{br}^2 \tag{1}$$

where $f_i(k)$ represents the sum of active power loss, br the sum of the network's branches, R_{br} the branch resistance, and I_{br} the branch current.

b. Average voltage deviation index (AVDI) minimization

$$f_{ii}(a) = \frac{1}{N_n} \sum_{z=1}^{N_n} |1 - V_z|^2 \tag{2}$$

Where $f_{ii}(j)$ is the AVDI, N_n is the sum of buses in the DN, V_z is the bus z's voltage.

c. Maximization of the Voltage stability index (VSI)

At a given end bus, z, the VSI is evaluated as:

$$\begin{aligned} f_{iii}(a) = [|V_z|^4 - 4(P_z x_{yz} + Q_z r_{yz})^2 \\ -4(P_z r_{yz} + Q_z x_{yz})|V_z|^2 \end{aligned} \tag{3}$$

Where V_z is bus z's voltage, P_z is bus k's active power, Q_z is node z's reactive power, r_{yz} is the resistance of the y-z branch, and x_{yz} is the impedance of the y-z branch.

Therefore, the multi-objective function is given by:

$$F(a) = \min\{w_1 f_i(a) + w_2 f_{ii}(a) - w_3 f_{iii}(a)\} \tag{4}$$

Where w_1, w_2, w_3 are initial weights.

2.6.2 Constraints

The multi-objective function is applicable when placing the EVCSs as well as when siz-

ing and siting the PV systems. Nevertheless, for both cases, the constraints slightly vary.

a. Equality constraints

- Power balance constraints for EVCSs

$$P_G = \sum_{k=1}^{N_n} P_l + \sum_{j=1}^{N_{EVCS}} P_{EVCS} + \sum_{i=1}^{br} P_{loss} \quad (5)$$

Where P_G represents the grid's active power, P_l the loads' active power demand, N_n the number of buses, P_{EVCS} the EVCSs active power demand, N_{EVCS} the number of EVCSs, P_{loss} the network active power loss, and N_{br} the network's total number of branches.

$$Q_G = \sum_{k=1}^{N_n} Q_l + \sum_{i=1}^{N_{br}} Q_{loss} \quad (6)$$

Where Q_G is the grid's reactive power, Q_l is the loads' reactive power demand, Q_{EVCS} is the EVCS reactive power demand, and Q_{loss} is the network reactive power loss.

- Power balance constraints for PV sizing and siting

$$P_G + \sum_{k=1}^{N_{pv}} P_{pv} = \sum_{k=1}^{N_n} P_l + \sum_{k=1}^{N_{EVCS}} P_{EVCS} + \sum_{k=1}^{N_{br}} P_{loss} \quad (7)$$

Where P_{pv} is the active power of a PV system.

$$Q_G + \sum_{k=1}^{N_{pv}} Q_{pv} = \sum_{k=1}^{N_n} Q_{load} + \sum_{k=1}^{N_{br}} Q_{loss} \quad (8)$$

Where Q_{pv} is the PV system's total reactive power.

b. Inequality constraints

- Bus voltage constraints

$$\begin{aligned} V_k^{min} &\le V_k \le V_k^{max} \\ 0.95 &\le V_k \le 1.05 \end{aligned} \quad (9)$$

- Current constraints

The current flowing through each feeder should not exceed the feeder's limits.

$$I_k \le I_k^{max} \quad (10)$$

- PV active power constraints

$$\begin{aligned} P_{pv}^{min} &\le P_{pv} \le P_{pv}^{max} \\ 100kW &\le P_{pv} \le 500kW \end{aligned} \quad (11)$$

- PV reactive power constraints

$$\begin{aligned} Q_{pv}^{\min} &\le Q_{pv} \le Q_{pv}^{\max} \\ 50\,\text{kVar} &\le Q_{pv} \le 200\,\text{kVar} \end{aligned} \quad (12)$$

2.7 Utilization of the Hybrid BFO-PSO

The hybrid BFO-PSO is utilized to integrate the EVCSs and to size and position the compensating PV systems.

2.7.1 Bacterial Foraging Optimization (BFO) algorithm

The BFO is an algorithm that was brought to life by K. M. Passino, who got inspiration from the "chemotaxis" activity of foraging bacteria like E. Coli [27]. The foraging activities of E. Coli that live in the human intestine are accomplished in the following steps: chemotaxis, swarming, reproduction, and elimination dispersal [28].

a. Chemotaxis: This is the process wherein the bacteria swim and tumble due to the movement of the flagella. For a single bacterium given by $\theta^k(l, m, n)$ at l^{th} chemotaxis, m^{th} reproduction, and n^{th} elimination-dispersal step, and unit of the run-length parameter $C(a)$, representing the step dimension of chemotaxis at every run, the bacterium's computational chemotactic displacement is represented as:

$$\theta^a(b+1, c, d) = \theta^a(b, c, d) + C(a)\frac{\Delta(a)}{\sqrt{\Delta^T(a)\Delta(a)}} \quad (13)$$

Where: Δ is a vector in any direction having elements in the set $[-1, 1]$.

b. Swarming: During swarming, the bacteria interact either attractively or repulsively

with the signals between them given by:

$$J_{cc}(\theta, P(b,c,d)) = \sum_{k=1}^{S} J_{cc}(\theta, \theta^a(b,c,d)) = \sum_{k=1}^{S} [-d_{attractant} \cdot \exp(-w_{attractant} \cdot \sum_{c=1}^{P} (\theta_c - \theta_c^i)^2)] + \sum_{k=1}^{S} [h_{repellant} \cdot \exp(-w_{repellant} \cdot \sum_{c=1}^{P} (\theta_c - \theta_c^i)^2)] \quad (14)$$

where $J_{cc}(\theta, P(b,c,d))$ is the objective function value, S is the bacteria population, p is every bacterium variable, $\theta = [\theta_1, \theta_2, \ldots, \theta_p]^T$ is a given point in the search domain, $d_{attractant}$, $w_{attractant}$ are depth and width attraction parameters and $h_{repellant}$, $w_{repellant}$ are height and width repulsion parameters.

c. Reproduction: Here, healthier bacteria asexually reproduce while the rest die. In so doing, the bacterial population is kept constant. Reproduction occurs at N_C step of chemotaxis, and it is expressed mathematically as:

$$J_{health}^i = \sum_{j}^{N_c+1} J(a,\ b,\ c,\ d) \quad (15)$$

d. Elimination and Dispersal: It happens at N_{re} reproduction steps, where something happens, and that leads to the sudden death or dispersal of the bacteria. P_{ed} is the likelihood that a bacterium will be put through elimination and dispersal, and P_e is the likelihood that some bacteria will be killed and the rest dispersed to another location for the process to repeat. N_{ed} is the sum of elimination and dispersal.

2.7.2 Particle Swarm Optimization (PSO)

Just like BFO, PSO is also a technique brought to life in 1995 by Kennedy and Eberhart, drawing inspiration from birds and fish behavior, and it is well-suited for optimizing nonlinear problems [29]. In PSO, two concepts exist: the global optimum g_{best} which is the swarm's optimum solution, and the local optimum p_{best} which is every particle's optimum solution. For a swarm made up of particles, P, there exists a position vector $X_i^t = (x_{i1}, x_{i2}, x_{i3}, \ldots, x_{in})^T$ and a velocity vector $V_i^t = (v_{i1}, v_{i2}, v_{i3}, \ldots, v_{in})^T$ at iteration t, for each particle i, part of the swarm. The position and velocity vectors of every particle are renewed at each iteration via the j dimension using equations(16) and(17):

$$V_{ij}^{t+1} = wV_{ij}^t + c_1 r_1^t \left(p_{best_{ij}} - X_{ij}^t\right) + c_2 r_2^t \left(g_j - X_{ij}^t\right) \quad (16)$$

$$X_{ij}^{t+1} = X_{ij}^t + V_{ij}^{t+1} \quad (17)$$

Where $i = 1,\ 2,\ 3,\ \ldots,\ P$, c_1 and c_2 are the acceleration factors, $j = 1,\ 2,\ 3,\ \ldots,\ n$, r_1^t and r_2^t are any numbers among 0 and 1, w is an initial weight used to balance the global as well as the local searches.

2.7.3 Hybrid BFO-PSO

Blending BFO with PSO was first done by Korani in 2008, utilizing the ability of PSO to interchange information among the particles and BFO's capacity to search for novel solutions by way of elimination and dispersal [30]. In Hybrid BFO-PSO, the unit length direction of the tumble behavior of every bacterium is decided upon by using the bacterium's global best position as well as its local best position. In every chemotaxis, an update of the direction of the tumble is determined using equation (18):

$$\varnothing(j+1) = w \cdot \varnothing(j) + c_1 \cdot r_1(P_{lbest} - P_{current}) + c_2 \cdot r_2(g_{lbest} - P_{current}) \quad (18)$$

Where P_{lbest} is each bacterium's best position and g_{lbest} is the bacteria's global best.

The flowchart of the hybrid BFO-PSO is shown in Fig. 4. The hybrid BFO-PSO pseudo code is as follows:

Step 1: Initialization of BFO-PSO parameters

- Dimension of solution space, d
- Sum of bacteria, S
- Sum of swarming, N_s

- Sum of elimination and dispersal, N_{ed}
- Sum of chemotaxis steps, N_c
- Sum of reproduction steps, N_{re}
- Probability of elimination and dispersal, P_{ed}
- Size of each step, $C(k)$
- Position vector, $\theta^k(b, c, d)$
- Inertia weight, ω
- Position vector $\theta^a(b, c, d)$ at l^{th} chemotaxis, m^{th} reproduction, and m^{th} elimination-dispersal step for i^{th} bacterium
- Velocity v^{th} of i^{th} bacterium
- PSO acceleration parameters, c_1, c_2
- PSO random numbers, r_1, r_2

Step 2: Update

- The fitness function value, $J(a, b, c)$ of k^{th} bacterium at l^{th} chemotaxis, m^{th} reproduction
- The global best position θ_{gbest} of the bacteria
- The best fitness function $J_{best}(a, b, c)$ found so far

Step 3: Reproduction loop, $k = k + 1$

Step 4: Chemotaxis loop, $a = a + 1$

For each bacterium, B, in the population:

(i) Calculate the fitness function $J(a, b, c)$

(ii) Let $J_{final} = J(a, b, c)$ as there is a likelihood of getting a better fitness

(iii) Tumble: Create an arbitrary vector $\Delta(i)$ with $-1 \leq \Delta(a) \leq 1$

(iv) Move: Let $\theta(a, b+1, c) = \theta(a, b, c) + C(i) \cdot \frac{\Delta(k)}{\sqrt{\Delta^T(k) \cdot \Delta(k)}}$

(v) Evaluate $J(a, b + 1, c)$

(vi) Swim: Considering that just the k^{th} bacterium is swimming with the others, stagnant:

- Let the swim length counter $x = 0$
- While $x < N_s$:
  If $J(a, b + 1, c) < J_{final}$ (Doing better?)
  Let $J_{final} = J(a, b+1, c)$ and $\theta(a, b+1, c) = \theta(b, c, d) + C(k) \cdot \frac{\Delta(a)}{\sqrt{\Delta^T(a) \cdot \Delta(a)}}$ Use the resulting $\theta(a, b + 1, c)$ to compute the new $J(k, l + 1, m)$ as done in step 4(v). Otherwise $x = N_s$. While loop ends.

Step 5: Modification with PSO

For $a = 1, 2, 3, 4, \ldots, S$:

- Update θ_{gbest} and $J_{best}(a, b, c)$
- Update the k^{th} bacterium's position and velocity as follows:
- $$V_{ae}^{new} = wV_{ae}^{new} + C_1\varphi_1\left(\theta_{best_{ae}} - \theta_e^{old}(b+1,\ c,\ d)\right)$$
- $$\theta_e^{old}(b+1,\ c,\ d) = \theta_e^{old}(b+1,\ c,\ d) + V_{ae}^{new}$$

Step 6: $Sr = \dfrac{S}{2}$

The bacteria Sr having the highest fitness function values, die while the other fifty percent of the population separates into two, with the new bacteria occupying the space of the dead bacteria.

Step 7: If $x < N_{re}$, signifying that the specified sum of reproduction steps is still a distance away; hence, return to Step 1. The next generation starts in the chemotaxis loop.

Table 4 shows the BFO-PSO parameters used in this work, which are a slight deviation from the empirical values used in [30], with the aim of the solution's speed and accuracy.

2.8 Simulation Scenarios

The optimization technique is formulated to

- Solve the placement of the EVCSs in the commercial DN, considering that EV users charge their EVs during peak load hours. That is 10 am to 3 pm.

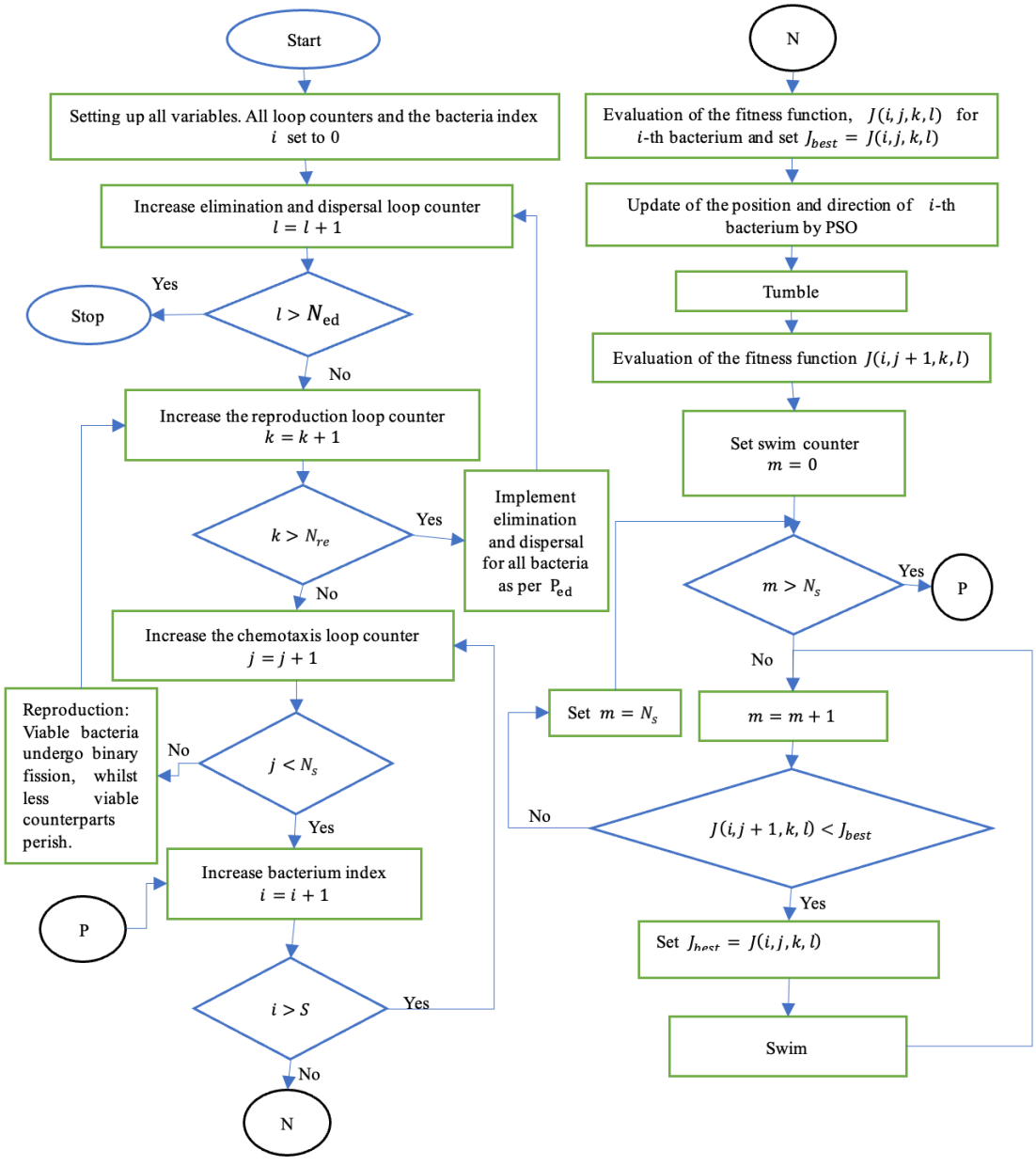

Fig. 4: BFO-PSO flowchart

Tab. 4: Simulation values for the hybrid BFO-PSO

Parameter	Value
Sum of bacteria, S	30
Sum of iterations	50
Chemotaxis steps, N_c	4
Swim steps, N_s	4
Reproduction steps, N_{re}	4
Sum of elimination and disposal, N_{ed}	2
Probability of elimination and disposal, P_{ed}	0.5
Highest inertia, w_{max}	4
Lowest inertia, w_{min}	-4
Acceleration vectors: c_1	0.02
c_2	0.02
Objective function weight: w_1	1
w_2	1
w_3	1

- Optimally sized and placed PV systems to alleviate the negative impact of the EVs on the DN during peak load hours, which also corresponds to peak sun hours, hence peak PV production hours.

3.0 Results and Discussions

3.1 Optimal EVCS allocation, and optimal sizes and sites of PV systems

Table 5 shows the best locations of the EVCSs, and the careful sizes and sites of the PVs as obtained by the BFO-PSO. Fig. 5 depicts the optimal locations of the EVCSs and PVs as picked by the BFO-PSO optimization technique. One can see that the EVCSs are placed not too far from the slack bus where grid power is injected. This permits the EVCSs to operate with an overall minimal network power loss, voltage deviation, and enhanced voltage stability since they are an extra load burden to the DN. At those locations, they stress the DN less. On the other hand, it is observed that the best nodes for the PVs are faraway buses. These are buses with the lowest voltages, especially buses 59 to 65, and therefore picked by the hybrid technique to place the PVs. Having the PVs at these weakest buses enhances the functionality and robustness of the DN. With this, the variations in the network voltage profile, voltage stability index (VSI) profile, minimum VSI, AVDI, and power losses in the network are presented and discussed.

3.2 Network voltage profile

The bus voltages of the DN without EVCSs and PV systems, with EVCSs only, and with EVCSs and PV systems, are shown in Fig. 6. The strategic allocation of the EVCSs by the BFO-PSO is very effective and only leads to a slight drop in some node voltages, mostly those from nodes 37 to 46, as shown in Fig. 7. These voltage drops are a result of the EVCSs being extra loads to the network. The introduction of the EVCSs slightly decreases the lowest node voltage of the network from 0.9287 p.u. experienced on node 65 to 0.9286p.u. Nevertheless, the hybrid optimization technique upgrades this voltage profile by accurately sizing and locating the compensating PVs in the network. It is viewed that the lowest node voltage with the incorporation of PVs is increased to 0.9493p.u., still on node 65, compared to 0.9286p.u with EVCSs. The compensating PV systems lead to an increase beyond 1p.u. of the node voltages of nodes 39 and 40 (1.001p.u.). This is still within the acceptable voltage margin. The PV systems can ameliorate the DN voltage profile because they are installed at the load centers where the energy is consumed, leading to a drop in the power demanded from the grid by both the EVCSs and the local loads.

3.3 AVDI and VSI

The AVDI, which is the measure of how far the average voltage of the network has deviated from the reference voltage (1p.u.), is slightly increased when the EVCSs are brought into the DN, as shown in Fig. 8. Nevertheless, the increase in the AVDI as a result of the EVCS is very minimal (from 0.020976p.u. to 0.021129p.u.). The fine sizing and placement of the PV systems ameliorate the AVDI by reducing it to 0.016282p.u.

On the other hand, the minimum VSI of the network is slightly reduced due to the EVCSs from 0.74372 to 0.74363. Also, the introduction

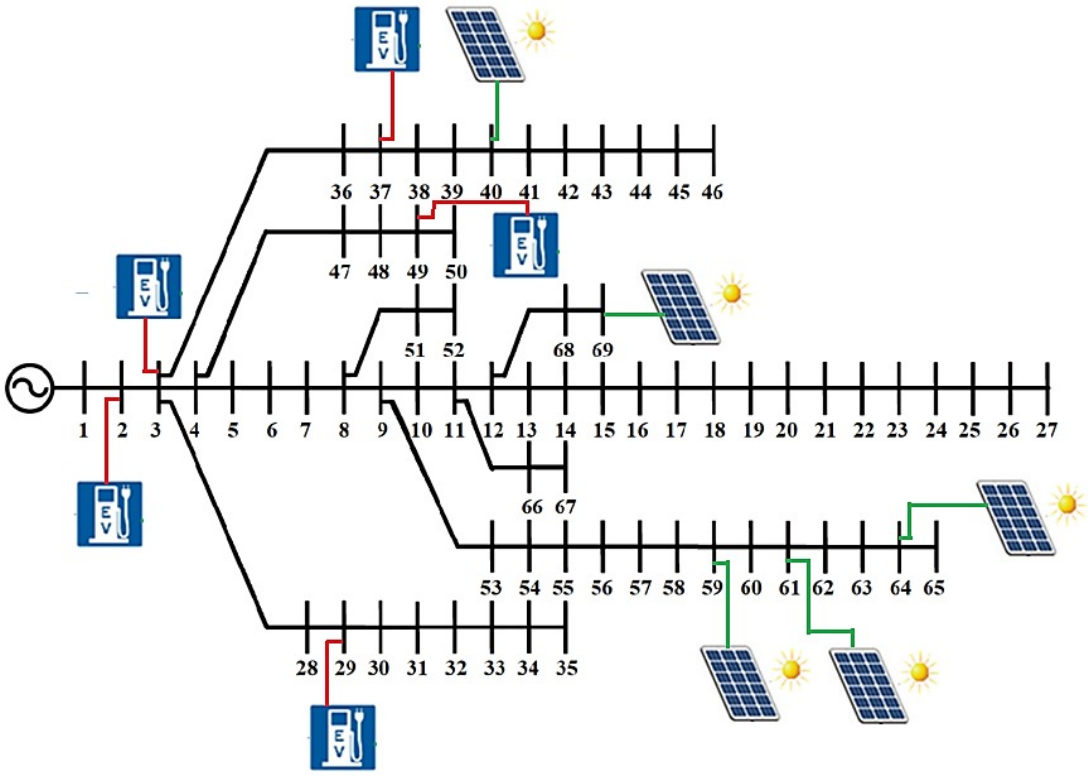

Fig. 5: Optimal locations of the EVCSs and PVs as found by the hybrid optimization technique

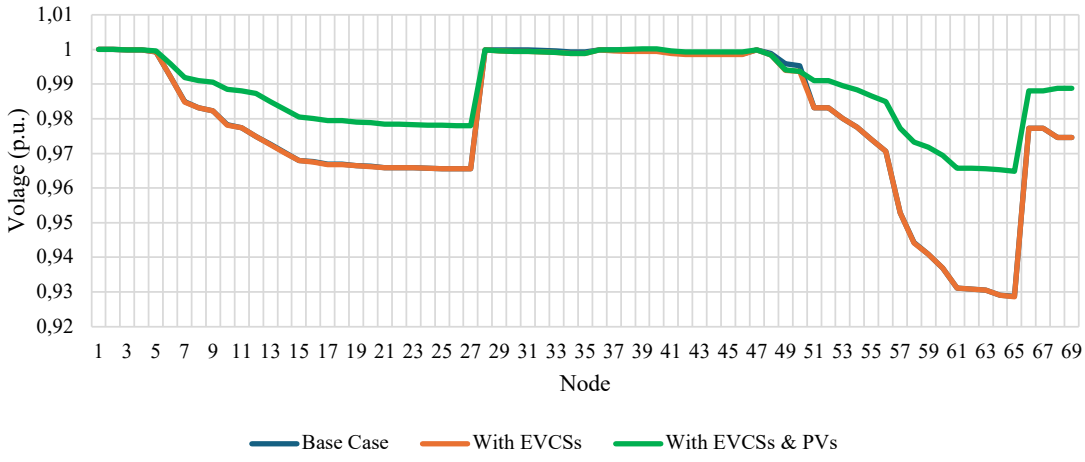

Fig. 6: DN voltage profile

Tab. 5: EVCS allocations and PV sizes, and sites

EVCS Rating (kW)	EVCS locations	Optimum PV Sizes		PV Location
		(kW)	(kVar)	
440	2	302	99.263	59
550	37	334	109.781	69
880	29	350	115.039	40
770	3	293	96.304	61
704	49	212	69.681	64

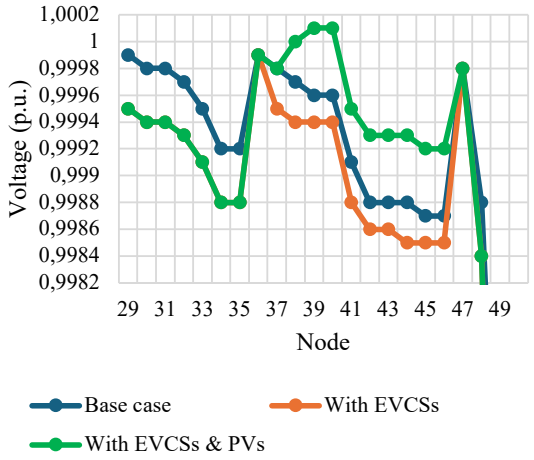

Fig. 7: Network voltage variations

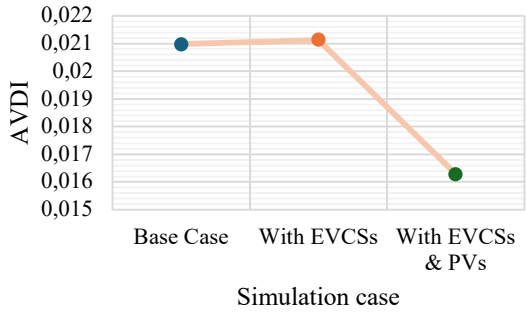

Fig. 8: Network's average voltage deviation index

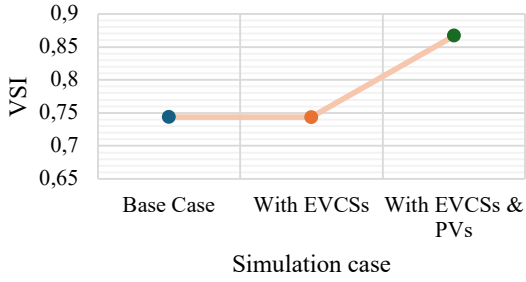

Fig. 9: Minimum voltage stability index

of the PV systems compensates for this drop in minimum VSI by raising it up to 0.86676, as shown in Fig. 9. VSI is an indication of how stable the network voltage is. The higher the VSI value, the less sensitive the network is to any voltage collapse and vice versa. On the other hand, the lower the AVDI, the closer the network operates to the reference voltage. The VSI profile of the network is shown in Fig. 10.

3.4 Power loss

The introduction of the EVCSs leads to a minor rise in active and reactive power losses from 138.8786 kW and 63.1915 kVar to 142.9875 kW and 73.2178 kVAr, respectively, as shown in Fig. 11. This is because, despite the virtue of the BFO-PSO in getting the finest locations for the EVCSs, the EVCSs remain additional loads to the network. Hence, this results in extra stress on the generating units to cater for the additional load demand and therefore extra power losses due to the increase in the feeders' current flow. It is noticed that the percentage increase in reactive power is 15.867%, and the percentage increase in active power is 2.959%. The choicest sizing and quintessential placement of the PVs drastically reduce the network power losses to 48.6442 kW, giving a percentage decrease of 65.98%, and 31.9676 kVAr, giving a percentage decrease of 56.34%, respectively. It is noticed that the power losses upon the integration of the compensative PV systems are far lower than the power losses in the base case, as

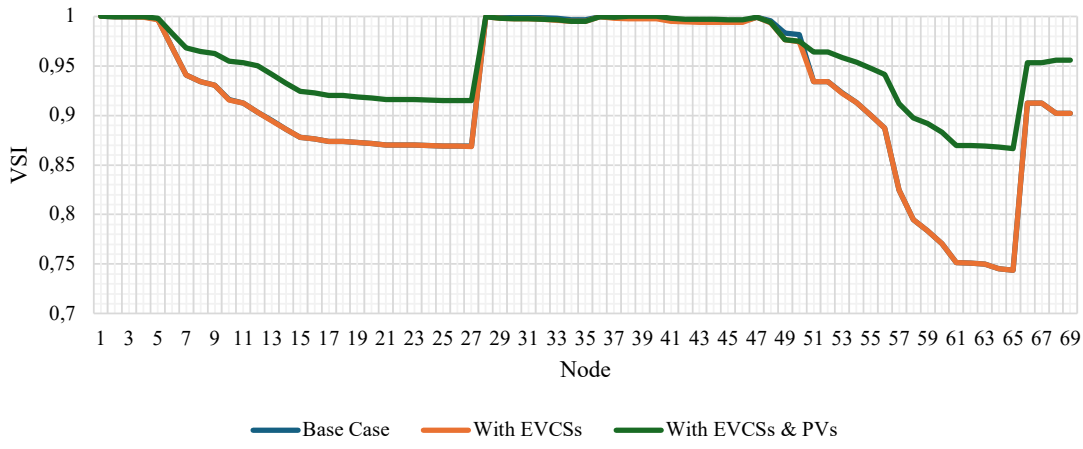

Fig. 10: Network Voltage Stability Index profile

shown in Figs. 11. This is accounted for by the fact that the PVs are installed directly at load centers where the power produced is consumed.

3.5 Validation of the Proposed Method in Placing EVCSs

To validate the supremacy of BFO-PSO for the allocation of EVCSs and PVs in the DN, its results are compared with those obtained when each optimization, PSO and BFO, is used standalone for the same task, as can be seen in Tables 6 and 7. From Table 6, it is seen that in the case of PSO, all five EVCSs are placed on the same bus (bus 5) of the DN, making the placement inefficient. This clustering of the EVCS on the same bus of the network could be due to PSO getting stuck in the local best, hence not getting to the global best solution. This problem is easily solved by hybridizing the PSO with BFO, as the chemotactic steps of the BFO prevent the PSO from being stuck in the local optimum solution, and therefore, the global best solution is obtained. Also, from Table 7, it is seen that for the total reactive power loss, the network parameters upon placing the EVCS using the hybrid BFO-PSO algorithm are better than when PSO and BFO are used separately. This proves the precedence of the hybrid algorithm over the standalone algorithms, as the hybrid algorithm uses the individual techniques' advantages to solve each other's disadvantages. The lowest voltage of the DN when using the hybrid algorithm is 0.9286p.u., which is higher than when using BFO (0.9253p.u.) and PSO (0.928p.u.) separately. Also, the resulting minimum VSI with BFO-PSO is 0.74363, and it is best compared to 0.73316 when using BFO and 0.74176 when using PSO. In addition to that, the AVDI of the network when the EVCS are placed using the proposed hybrid algorithm is 0.02113, which is best compared to 0.02293 when BFO is used and 0.02135 when PSO is used. In all, it is logical to substantiate the supremacy of the BFO-PSO in looking for the finest buses for the allocation of the five EVCS.

Tab. 6: Optimal location of the EVCS using the various optimization algorithms

EVCS rating (kW)	Optimal location of the EVCS under different algorithms		
	Hybrid BFO-PSO	BFO	PSO
440	2	53	5
550	37	29	5
880	29	38	5
770	3	47	5
704	49	39	5

Tab. 7: Network Parameters following the placement of EVCSs using various techniques

Algorithm	Min. volt	kW loss	kVar loss	Min VSI	AVDI
BFO	0.9253	158.049	77.764	0.73316	0.02293
PSO	0.928	143.701	69.31	0.74176	0.02135
BFO-PSO	0.9286	142.99	73.22	0.74363	0.02113

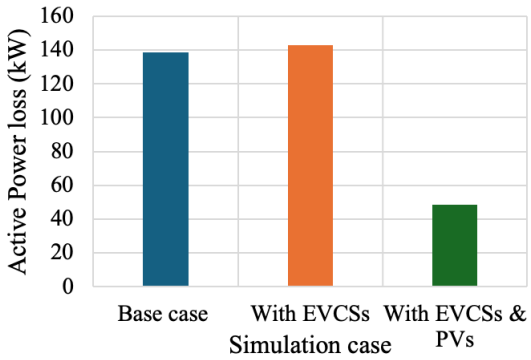

(a) Total active power loss

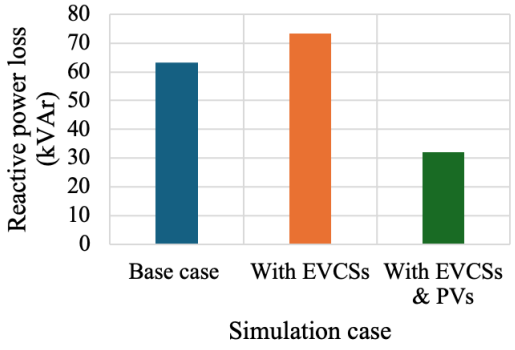

(b) Total reactive power loss

Fig. 11: Network total power loss

4.0 Conclusions

The incorporation of EVCSs into the DN to service the rising number of EVs in today's transport sectors needs to be done strategically to reduce the adverse effect the EVCSs could have on the electrical DN. This work proposed the hybrid BFO-PSO, which used PSO's potential to interchange information amongst the particles as well as BFO's capacity to search for novel solutions for the strategic allocation of EVCSs and compensating PV systems into the DN. The optimization challenge was described as a multi-objective one that maximized the voltage stability index while minimizing power loss and the average voltage deviation index. The proposed method was put to the test on the standard IEEE 69-node test DN, considered a purely commercial network. Using MATLAB 2019a, the simulation was done, and the proposed method demonstrated its effectiveness in looking for the finest positions for the EVCSs and the best sizes and locations for the compensating PV systems while observing the set optimization constraints. Minimal voltage drops were noticed due to the EVCSs, and these were adequately compensated by the PV systems. Likewise, the rise in power losses as a consequence of the EVCSs was sufficiently compensated for by the PV systems. This work could be a stepping stone to the strategic integration of EVCSs into the DN, which is crucial for distribution network operators as it helps balance electricity demand, avoids equipment overload, and saves money on expensive infrastructure upgrades. Furthermore, the operators may better integrate renewable energy, spread out power use, and preserve grid dependability. This will help the network stay resilient and efficient as EV usage increases. On the other hand, optimal EVCS allocation benefits town planners as it helps them maximise economic and sustainability benefits, boosts local economies, while seamlessly integrating with transportation and urban development plans.

Given that this study does not take into consideration dynamic parameters such as EV charging time, amongst others, the next step of this work envisages diving into the driving pattern of EV users, the EV battery's state of charge, and the charging time. Also, the impact of daily temperature variation on PV production will be considered.

References

[1] M. A. Farahani and M. Haeri. Hierarchical event-triggered online charging management of time-varying network of electric vehicles based on cooperative game theory. *Majlesi J. Electr. Eng.*, 18(1):75–89, 2024.

[2] M. Moradijoz and M. P. Moghaddam. Optimum allocation of parking lots in distribution systems for loss reduction. In *2012 IEEE Power and Energy Society General Meeting*, pages 1–5. IEEE, 2012.

[3] W. Ejaz, M. Naeem, M. R. Ramzan, F. Iqbal, and A. Anpalagan. Charging infrastructure placement for electric vehicles: An optimization prospective. In *27th International Telecommunication Networks and Applications Conference (ITNAC)*, pages 1–6. IEEE, 2017.

[4] R. Puliti. In developing countries, the e-mobility revolution is closer than you might think. world bank blog, 2022.

[5] Y. Xiong, J. Gan, B. An, C. Miao, and A. L. C. Bazzan. Optimal electric vehicle fast charging station placement based on game theoretical framework. *IEEE Trans. on Intell. Transp. Syst.*, 19(8):2493–2504, 2017.

[6] A. Rajabi-Ghahnavieh and P. Sadeghi-Barzani. Optimal zonal fast-charging station placement considering urban traffic circulation. *IEEE Trans. on Veh. Technol.*, 66(1):45–56, 2016.

[7] S. Faddel, A. T. Al-Awami, and O. A. Mohammed. Charge control and operation of electric vehicles in power grids: A review. *Energies*, 11(4):701, 2018.

[8] U. C. Chukwu and S. M. Mahajan. Real-time management of power systems with v2g facility for smart-grid applications. *IEEE Trans. on Sustain. Energy*, 5(2):558–566, 2013.

[9] M. Daneshvar, M. Abapour, B. Mohammadi-Ivatloo, and S. Asadi. Impact of optimal dg placement and sizing on power reliability and voltage profile of radial distribution networks. *Majlesi J. Electr. Eng.*, 2019.

[10] M. J. Kasaei and J. Nikoukar. Dg allocation with consideration of costs and losses in distribution networks using ant colony algorithm. *Majlesi J. Electr. Eng.*, 10(1), 2016.

[11] K. P. Tiwari and K. Thakre. Control of hybrid standalone power supply system using artificial neural network. *Majlesi J. Electr. Eng.*, 19(1):1–9, 2025.

[12] O. A. Odetoye, O. Oghorada, A. O.Alimi, B. Adetokun, U. N. Okeke, J. O. O., P. K. Olulope, and M. O. Olanrewaju. Impact of the penetration of renewable energy on distributed generation systems. *Majlesi J. Electr. Eng.*, 16(4), 2022.

[13] O. Garfi, H. Aloui, and N. Chaker. Impacts of photovoltaic power source intermittence on a distribution network. *Int. J. Electr. Comput. Eng.*, 9(6):5134, 2019.

[14] P. Chiradeja. Benefit of distributed generation: A line loss reduction analysis. In *2005 IEEE/PES Transmission & Distribution Conference & Exposition: Asia and Pacific*, pages 1–5. IEEE, 2005.

[15] P. V. K. Babu and K. Swarnasri. Multi-objective optimal allocation of electric vehicle charging stations in radial distribution system using teaching learning based optimization. *Int. J. Renew. Energy Res.*, 10(1):366–377, 2020.

[16] E. A. Rene, W. S. T. Fokui, and P. K. N. Kouonchie. Optimal allocation of plug-in electric vehicle charging stations in the distribution network with distributed generation. *Green Energy Intell. Transp.*, 2(3):100094, 2023.

[17] M.Z. Zeb, , K. Imran, A. Khattak, A.K. Janjua, A. Pal, M. Nadeem, J.Zhang, and S.Khan. Optimal placement of electric vehicle charging stations in the active distribution network. *IEEE Access*, 8:68124–68134, 2020.

[18] S. Pazouki, A. Mohsenzadeh, M.-R. Haghifam, and S. Ardalan. Simultaneous allocation of charging stations and capacitors in distribution networks improving voltage and power loss. *Can. J. Electr. Comput. Eng.*, 38(2):100–105, 2015.

[19] S. K. Injeti and V. K. Thunuguntla. Optimal integration of dgs into radial distribution network in the presence of plug-in electric vehicles to minimize daily active power losses and to improve the voltage profile of the system using bio-inspired optimization algorithms. *Prot. Control. Mod. Power Syst.*, 5(1):1–15, 2020.

[20] S. D. Nugraha, M. Ashari, and D. C. Riawan. Multi-objective approach for optimal sizing and placement of evcs in distribution networks with distributed rooftop pv in metropolitan city. *IEEE Access*, 2025.

[21] M. Bilal, M. Rizwan, I. Alsaidan, and F. M. Almasoudi. Ai-based approach for optimal placement of evcs and dg with reliability analysis. *IEEE Access*, 9:154204–154224, 2021.

[22] S. Deb, K. Tammi, X. Gao, K. Kalita, and P. Mahanta. A hybrid multi-objective chicken swarm optimization and teaching learning based algorithm for charging station placement problem. *IEEE Access*, 8:92573–92590, 2020.

[23] O. D. Montoya, W. Gil-Gonzalez, and A. Garces. On the conic convex approximation to locate and size fixed-step capacitor banks in distribution networks. *Computation*, 10(2):32, 2022.

[24] M. S. Elnozahy and M. M. A. Salama. Studying the feasibility of charging plug-in hybrid electric vehicles using photovoltaic electricity in residential distribution systems. *Electr. Power Syst. Res.*, 110:133–143, 2014.

[25] K. Muchiri, J. N. Kamau, D. W. Wekesa, C. O. Saoke, J. N. Mutuku, and J. K. Gathua. Solar pv potential and energy demand assessment in machakos county. *MksU Press*, 2019.

[26] E. Hadian, H. Akbari, M. Farzinfar, and S. Saeed. Optimal allocation of electric vehicle charging stations with adopted smart charging/discharging schedule. *IEEE Access*, 8:196908–196919, 2020.

[27] H. Chen, Y. Zhu, and K. Hu. Adaptive bacterial foraging optimization. *Abstr. Appl. Anal.*, 2011(1):108269, 2011.

[28] S. M. Abd-Elazim and E. S. Ali. A hybrid particle swarm optimization and bacterial foraging for optimal power system stabilizers design. *Int. J. Electr. Power & Energy Syst.*, 46:334–341, 2013.

[29] B. Seixas Gomes de Almeida and V. Coppo Leite. Particle swarm optimization: A powerful technique for solving. *Swarm intelligence: Recent advances, new perspectives applications*, pages 1–21, 2019.

[30] T. Zang, Z. He, and D. Ye. Bacterial foraging optimization algorithm with particle swarm optimization strategy for distribution network reconfiguration. In *International Conference in Swarm Intelligence*, pages 365–372. Springer, 2010.

About Authors

Willy Stephen Tounsi FOKUI is a philomath who has been working as a Hardware Development Engineer at Teleconnect GmbH, Dresden, Germany since March 2023. He holds a Ph.D. in Electrical Engineering (Power Systems), defended in April 2022 at the Pan African University Institute for Basic Sciences, Technology and Innovation (PAUSTI), hosted at Jomo Kenyatta University of Agriculture and Technology, Nairobi, Kenya. His Master's and Bachelor of Engineering both in Power Systems were acquired in 2017 and 2014, respectively, at the University of Buea, Cameroon. Willy is a researcher with over 24 publications in quality journals and conference proceedings. In addition to being a devoted engineer, Willy is a researcher with over 24 publications in quality journals and conference proceedings. His interests include, amongst others, analogue and mixed signal design, digital circuit design, industrial and automotive electronics, System on Chip (SoC) design, AC/DC and DC/DC power supply designs, wireless power transmission, optical transceiver design, and sustainable energy

Ebunle Akupan RENE is a dedicated research fellow and holds a Bachelor of Engineering and a Master of Engineering in Electrical and Electronic Engineering (Power system option), both obtained from the University of Buea, Faculty of Engineering and Technology, Cameroon. Ebunle has served as a university instructor for over five years. Ebunle's research endeavors have resulted in publications, covering a diverse range of topics like optimal control theories, electric vehicle charging station integration, load frequency control, optimal AC-DC PV-Hydro power modeling for microgrid applications, FACTS devices, and predictive controls. Ebunle's research interests include power electronics, adaptive controls, electric vehicles, renewable energy, Reinforcement learning, and optimization. His focus on these areas demonstrates his commitment to innovation in the field.

Danube Kirt Ngongang WANDJI is a Research Fellow, Data Science and Air Quality Management at SEI Africa. He is an air quality analyst with diverse research background in energy efficiency in built environment with a focus on clean energy solutions to address the lighting and cooking needs for municipalities including in informal settlements, and inclusive frontier technologies to improve access, coverage and quality of basic services such as energy, water and sanitation, and air quality data management. Ngongang holds an MSc. in Electrical Engineering (Telecommunication Option) from the Jomo Kenyatta University of Agriculture and Technology (JKUAT) in Kenya, where he was a recipient of an African Union Commission Scholarship, and a BSc. in Electronics and Electrical Engineering from Obafemi Awolowo University in Nigeria. A native of Cameroun, he is fluent in French and English.